Pharmaceutical Research, Vol. 26, No. 2, February 2009 (© 2008)
DOI: 10.1007/s11095-008-9750-9

Research Paper

Colloidal Structures in Media Simulating Intestinal Fed State Conditions with and Without Lipolysis Products

Dimitrios G. Fatouros,[1,3] Isabelle Walrand,[1] Bjorn Bergenstahl,[2] and Anette Müllertz[1]

Received April 18, 2008; accepted October 6, 2008; published online November 12, 2008

Purpose. To study the ultrastructure of biorelevant media and digestion products of self-nanoemulsifying drug delivery system (SNEDDS) at high level BS/PL conditions.
Methods. Cryogenic transmission electron microscopy (Cryo-TEM) was employed to visualize the colloid structures in the biorelevant media and lipolytic products generated during hydrolysis of a SNEDDS formulation. Their electrical properties were investigated by measuring their ζ-potential values.
Results. In the biorelevant media, vesicles (either unilamellar or multilamellar) and bilayer fragments are visualized. Occasionally, vesicles with an internal deformed structure are recognized, suggesting surface tension or uneven lateral stress. Visualization studies of the intermediate colloidal phases produced during digestion of a SNEDDS using the *in vitro* lipolysis model revealed the formation of similar structures as previously reported. The ζ-potential of the media was negatively charged and decreased from −23 to −35 mV with increasing surfactant/lipid load. Lower ζ-potential values (−16 mV) obtained for the structures formed during the lipid hydrolysis of the SNEDDS were probably due to the presence of calcium, which shields the surface, thereby reducing the charge.
Conclusions. The diversity of these vesicles in terms of size, lamellarity, and internal organization advocate their important role during lipid digestion in the gastrointestinal milieu.

KEY WORDS: ζ-potential; biorelevant media; cryogenic transmission electron microscopy; *in vitro* digestion lipolysis model; lipolytic products; micelles; multilamellar vesicles; self-nanoemulsifying drug delivery systems; unilamellar.

INTRODUCTION

Small intestinal fluid contains various endogenous surfactants, including bile salts (BS) and phospholipids (PL), which form mixed micelles with high solubilizing capacity for many poorly soluble drugs (1–6). Human intestinal BS concentrations reported in the literature are dependent on many factors (e.g. site and sampling time with regard to meals and composition of the meal). In general, mean fasted state BS concentrations typically range from 1.5 to 6 mM (7,8), while mean postprandial concentrations typically range from 8 to 20 mM with values as high as 40 mM having been reported (9–12). Phase distribution studies of *in vivo* aspirates sampled from duodenum during digestion have previously demonstrated that unilamellar vesicles coexist with micelles (13,14).

Biorelevant dissolution media, simulating the intestinal fluids, containing BS and PL have been used for solubility studies of poorly soluble drugs for oral administration. Several studies have demonstrated a correlation between drug lipophilicity and improved compound solubility in biorelevant media relative to the corresponding intrinsic water solubility (15–18). Addition of FA and MG, which are formed during digestion of triglycerides, can simulate the fed state.

During lipid digestion, the trafficking of a particular drug substance between these various colloid phases will be controlled by several factors, many of which are poorly understood, but are thought to include the drug lipophilicity and affinity for the various lipid phases (19,20). Recently, it has been demonstrated that the intermediate phases produced during lipid digestion can play a significant role in the drug solubilization and trafficking in the gastrointestinal tract, thereby influencing the overall performance of the formulation (19). Despite very encouraging results from solubilization studies in the presence of lipolytic products, the mechanism of action of these media is still not fully understood. In light of this, characterization of such media can offer important information on the role of intermediate phases of lipid digestion and drug solubilization in the gastrointestinal tract.

For that purpose, a series of biorelevant media containing bile salt (BS, sodium taurocholate), phosphatidylcholine (PL), with fatty acids (FA, oleic acid) and monoglycerides (MG, monoolein) were developed. Constant ratios of BS to PL (4:1) representing intestinal contents after digestion of a formulation under high BS and PC conditions were employed

[1] Department of Pharmaceutics and Analytical Chemistry, The Faculty of Pharmaceutical Science, University of Copenhagen, Universitetsparken 2, 2100, Copenhagen, Denmark.
[2] Department of Food Technology, Center for Chemistry and Chemical Engineering, Lund University, P.O. Box 12422100, Lund, Sweden.
[3] To whom correspondence should be addressed. (e-mail: df@dfuni.dk)

and the pH was fixed at 6.5. The ratio between MG: FA was 1:2 which stoichiometrically corresponds to the amount of MG and FA produced during the hydrolysis of triacylglycerols (21).

Cryogenic transmission electron microscopy (Cryo-TEM) was used to investigate the structural characteristics of the media. Previously, vitreous ice Cryo-TEM has proven to be an excellent tool to provide insight on the mechanisms of the interactions between vesicles and micelles (22,23). The advantage of Cryo-TEM is the avoidance of any fixation of the sample grid, which can create artifacts induced by staining, and thus keeps the sample close to the original state (24,25). During that process, a thin layer of the sample is rapidly frozen by plunging it into liquid ethane at −180°C to achieve a cooling rate fast enough to prevent rearrangement of molecules into another form. Moreover, absence of any staining eliminates the risk of extraction of lipid material during the fixation of the sample.

The *in vitro* digestion of a self-nanoemulsifying drug delivery system (SNEDDS) in the fed state was visualized by Cryo-TEM. The dynamic lipolysis model, simulating the environment of the gastrointestinal tract in high level BS and PL conditions, was used for this purpose (26,27).

The intermediate phases generated during lipid digestion have been previously studied by light microscopy (28,29) or freeze fracture electron microscopy (30,31). These studies focus on digestion of dietary lipids, and not on pharmaceutical lipid based formulation. Recently, we have demonstrated that Cryo-TEM coupled with the *in vitro* lipolysis model can be a very useful tool for monitoring structural changes of pharmaceutically relevant formulations (SNEDDS; 32).

The aim of the current study was to investigate the effect of the composition of different biorelevant media containing bile components and lipolytic degradation products on their electrical properties and morphology and to compare with colloid structures generated during *in vitro* digestion of a SNEDDS at similar conditions at high level BS and PL conditions.

MATERIALS AND METHODS

Materials

Oleic acid, sodium taurocholeate, cholesterol, sodium chloride, sodium azide and trizma maleate were purchased from Sigma (St. Louis, MO). PL (S100 containing approximately 94% PC) was kindly donated from Lipoid GmbH (Ludwigshafen, Germany). Danisco (Denmark) generously donated glycerol monoolate (Monoolein). Pancreatin (porcine), bile extract (porcine), sesame oil and trizma maleate, were purchased from Sigma-Aldrich (USA). 4-Bromobenzeneboronic acid (BBBA) was purchased from Lancaster (Germany). Cremophor RH 40 was purchased from BASF (Germany) and maisine 35-1 (containing glyceryl monolinoleate) from Gattefossé (France) respectively. The water used was obtained from a Milli-Q-water purification system manufactured by Millipore (USA.) All other chemicals were of analytical grade.

Preparation of Biorelevant Media

The composition of biorelevant media is presented at Table I. Combinations of sodium taurocholate (bile salt, BS), lecithin (phospholipid, PL), monoolein (monoglyceride, MG) and oleic acid (fatty acid, FA) were prepared at different ratios. The osmolarity of buffer solution was fixed at 270 mOsmol/Kg, included 100 mM trizma maleate at pH 6.5, and contained either 65.1 mM or 59.5 sodium chloride. To prevent microbial growth 3 mM of sodium azide were added.

The biorelevant media were prepared by weighting the exact amounts of the components. Buffer solution was added to give the desired molar ratios and left for 24 h under stirring at 37°C. Each medium was prepared in triplicate. The notations used for the media were the Latin numbers from I to IV. Medium I, containing only sodium taurocholate and lecithin, served as a control.

Preparation of Self-Nanoemulsifying Drug Delivery System (SNEDDS)

A previously developed SNEDDS formulation was used in this study (33). The SNEDDS consisted of a mixture of long chain triglycerides (sesame oil; 30% *w*/*w*), mono-, di-, and triacylglycerides, maisine 35-1 (30% *w*/*w*), Cremophor RH 40 (30% *w*/*w*), and ethanol (10% *w*/*w*) acting as a co-solvent.

Lipolysis Model

An established *in vitro* lipolysis model was employed to characterize the lipid-based formulation (27). In brief, the experimental set-up consisted of a thermostated (37°C) reaction vessel, a pH-stat (pH 6.5) with auto burette for the addition of sodium hydroxide (NaOH), and a peristaltic pump for the addition of 0.5 M Ca^{2+} solution with a dispensing rate of 0.045 mmol/min.

The pH was set at 6.5 as a compromise between the optimum for the pancreas lipase, which is between 6 and 10 (34) and the measured duodenal pH, which is around 5.0–5.5 during a test meal (35,36).

Table I. Composition of Biorelevant Media

Biorelevant media	Sodium taurocholeate (mM)	Lecithin (mM)	Monoolein (mM)	Oleic acid (mM)
I[a]	15	3.75		
II[a]	15	3.75	7.5	15
III[b]	15	3.75	10	20
IV[b]	20	5	10	20

[a] In media I and II the sodium chloride concentration was 65.1 mM
[b] In media III and IV the sodium chloride concentration was 59.5 mM

The experiment was performed under continuous agitation obtained by magnetic stirring (100 rpm) and the total volume of the medium was 300 mL. The number of OH^- ions present in the volume of the titrant could be equated with the fatty acid liberation caused by lipolysis.

A concentration of 20 mM of bile salts [BS] and 5 mM of phosphatidylcholine [PL] was used to simulate the fed conditions in the gastrointestinal tract (13). The initial composition of the lipolysis medium used in this study is shown in Table II. The SNEDDS consisted of a mixture of long chain triglycerides (LCT): sesame oil (30% *w*/*w*), triacylglycerides (primarily oleic and linoleic acid), maisine 35-1 (30% *w*/*w*) containing mainly mono- and diacylglycerides (primarily containing oleic and linoleic fatty acids), Cremophor RH 40 (30% *w*/*w*), and ethanol (10% *w*/*w*) acting as a co-solvent. Three grams of the respective formulation was added to the medium and equilibrated before the lipolysis process was initiated by adding the lipase solution. At specific time points (0, 2, 5 and 30 min), 10 mL samples were taken and the lipase activity was inhibited immediately (4-bromobenzeneboronic acid solution).

The lipase solution was prepared in accordance with a previously described method (27) to give an activity of 800 USP units/ml. Briefly 16.6 g of pancreatin was weighted accurately, suspended in 110 ml of Millipore water at 37°C and mixed thoroughly. The suspension was centrifuged for 7 min at 4000 rpm and 37°C while 1.00 M NaOH was used to adjust the pH of the supernatant to 6.5. Then 100 mL of the supernatant were added to the lipolysis medium. The time spent on preparing the solution did not exceed 15 min in order to minimize denaturation. The lipase activity of pancreatin was determined in accordance with USP 26 2003 (37).

ζ-Potential Determinations of Biorelevant Media and Lipolytic Products

The electrophoretic mobility of the colloidal structures formed in the biorelevant media as well as during *in vitro* lipid digestion was measured at 37°C with a Zetasizer (Malvern Nanosizer ZS, Malvern Instruments, UK). The ζ-potential of the dispersions was calculated by the instrument according to the Helmholtz–Smoluchowski equation. ζ-potential determinations were performed in triplicate from three different formulations.

Statistical Analysis

The results have been expressed as the mean±standard deviation. Statistical comparisons were made using *t* test. The probability value of less than 0.05 was considered to be significant.

Table II. Composition of the Lipolysis Medium

Substance	Initial concentration
BS	20 mM
PL	5 mM
Pancreatic lipase	800 USP units/ml
Trizma-maleate	2 mM
Na^+	150 mM
Ca^{2+}	0.045 mmol/min
Total volume	300 mL

Cryo-TEM Studies

The samples for the Cryo-TEM studies were prepared in a controlled environment vitrification system (CEVS). A small amount of the sample (5 μL) was put on carbon film supported by a copper grid and blotted with filter paper to obtain a thin liquid film on the grid. The grid was quenched in liquid ethane at −180°C and transferred to liquid nitrogen (−196°C). The samples were characterized with a TEM microscope (Philips CM120 BioTWIN Cryo) equipped with a post column energy filter (GATAN GIF 100) using Oxford CT3500 cryoholder and its workstation. The acceleration voltage was 120 kV and the working temperature was −180°C. The images were recorded with a CCD camera (Gatan 791) under low dose conditions. The defocus was approximately 1 μm.

RESULTS AND DISCUSSION

Fed State Biorelevant Media

ζ-Potential of Structures in Fed State Biorelevant Media

The relation between the total concentration of anionic species and the ζ-potential values are illustrated in Fig. 1. The ζ-potential measurements reveal that all media possess a negative surface charge. Overall, the changes to the ζ-potential of the media are determined by the relative contribution of each component separately. As previously demonstrated, BS and FA possess a negative charge (38,39), while PL head groups are zwitterionic with no net charge at this pH range (40). On the other hand, monoolein is a neutral lipid with a ζ-potential value of zero (41).

Medium IV (containing 20 mM BS and 20 mM FA) possess the highest ζ-potential values in absolute numbers (−35.03 mV) compared with media II and III media (both containing 15 mM BS, but 15 and 20 mM FA respectively) having ζ-potential values of −32.00 and −33.20 mV respectively (Fig. 1). However, these values are not significantly different (*t* test $p>0.05$). In contrast, medium I containing only BS (15 mM) and PL had significantly lower zeta potential values (−23.0 mV; *t* test $p<0.01$).

Cryo-TEM Analysis of Biorelevant Media

The images presented in this study are a representative selection of 152 images in total. Fig. 2 illustrates micelles, as black "dots", containing sodium taurocholeate and lecithin representing intestinal contents of a formulation under high BS and PL conditions (BS/PL 15:3.75). Previously, studies of similar media (BS/PL 20:5) revealed mean diameters up to 7 nm as measured by photon correlation spectroscopy (19). This is in broad agreement with the results obtained in the current study. Representative Cryo-TEM images of medium II are illustrated in Fig. 3. Unilamellar and bilamellar vesicles with an internal deformed structure are recognized. Micelles and bilayer fragments are also detected. The unilamellar and bilamellar vesicles with a diameter up to 100 nm are depicted in Fig. 3a–c. The diameter of the unilamellar vesicles is less than 50 nm. This is in contrast with the bilamellar vesicles that exceeded diameters up to 100 nm. A ruptured bilamellar (indicated by the black arrow) and an open bilamellar vesicle

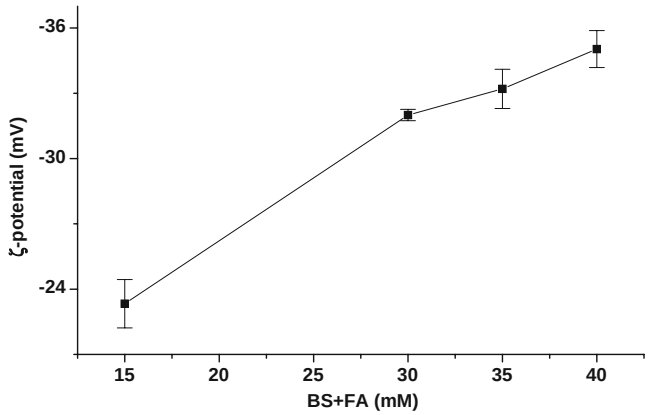

Fig. 1. ζ-potential values as a function of lipid material. All measurements performed at 37°C. These are the mean values±SD of three different experiments.

are depicted in Fig. 3c (indicated by the yellow arrow). The observed opening in the vesicle might be related to the presence of the bile salts in the medium. Bile salts can create pores in lipid membranes (42). Release studies of small solutes (e.g. carboxyflouroscein) are consistent with the theory that transient and rapid-releasing membrane holes form after bile salt addition (43,44). Such openings in the membranes, visualized by Cryo-TEM, were previously observed when phosphatidylcholine vesicles were incubated with bile salts (24). The formation of open vesicles was attributed to the creation of such pores on the bilayers. The presence of open vesicles supports the hypothesis for lipid fragments since they can be considered lipid aggregates originating from lamellar structures. Indeed, bilayer fragments are occasionally spotted (Fig. 3a–c; (indicated by white arrows).

When the colloid structures exceeded in diameter the value of 100 nm, vesicles containing internal deformed structures were observed (Fig. 3d,e). Moreover, undulations and ripples are present on the bilayers in the inner part of the vesicles (indicated by black arrows). The uneven morphology of these bilayers advocates that the formation of such structures is a dynamic process. The long bilayer fragment, located closely to a vesicle (Fig. 3d, indicated by white arrow), implies that a process is in progress. Generally, open vesicles and the breakdown of vesicles into bilayer fragments indicate the first step towards the transition from vesicles to micelles (45). Interestingly, in one instance a multi-compartment vesicle was observed (Fig. 3e, indicated by white arrow).

In all cases the vesicles appear non-aggregated. This can be explained from their high ζ-potential values (Fig. 1), suggesting repulsive interactions among them. Thus, vesicle stability can be increased by the addition of charged molecules that cause repulsion forces, thereby preventing vesicle fusion.

Medium III only differs from medium II by containing a 1.3 times higher concentration of FA and MG. As a consequence, there are no major differences between the structures in medium II and medium III. The formation of vesicles containing deformed internal structures are dominating structural features in medium II as well (Fig. 4a, indicated by black arrow). A disrupted vesicle membrane is also visible (Fig. 4a, indicated by white arrow).

Elongated vesicles are depicted as well (Fig. 4b,c, indicated by yellow arrows). Previously, it has been shown that vesicles containing anionic lipids such as Dioleylphosphatidylethanolamine (DOPE) and Dioleylphosphatidylcholine (DOPC) can form non-spherical geometries attributed to the negative charge of PE (46). The fact that these vesicles are negatively charged could support the hypothesis for the formation of such structures. A multivesicular structure with rippled bilayers is depicted at Fig. 4c (indicated by black arrow). Finally, unilamellar vesicles measuring less than 100 nm were present at low numbers (Fig. 4d).

Fig. 5 depicts the Cryo-TEM images of colloidal structures present in medium IV. Medium IV contains a higher level of BS and PL compared with the other media, but at the same molar ratio. The level of FA and MG corresponds to the level in medium III.

Dominating structures are unilamellar vesicles with diameter less than 40 nm in most cases (Fig. 5a,b). In comparison to medium II, less bilayer fragments were noticed. Bi-lamellar or tri-lamellar vesicles were observed as well (Fig. 5b). Multi-compartment vesicles (Fig. 5d, indicated by black arrow) with bilayer fragments or vesicles (Fig. 5d, indicated by white arrow) or cluster of vesicles

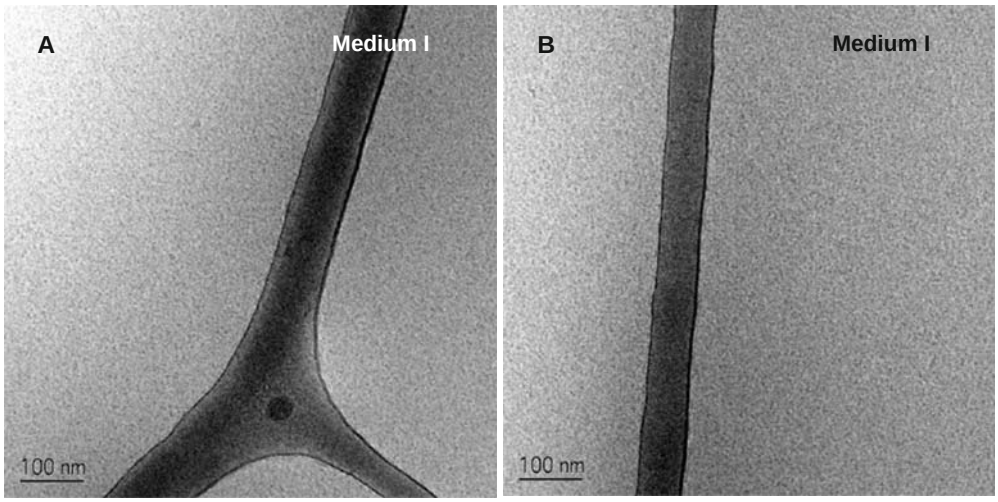

Fig. 2. Cryo-TEM micrographs of biorelevant media. All micrographs are taken from medium I (BS/PL, 15:3.75). Micelles depicted are as *black dots* are present. Scale bar represents 100 nm.

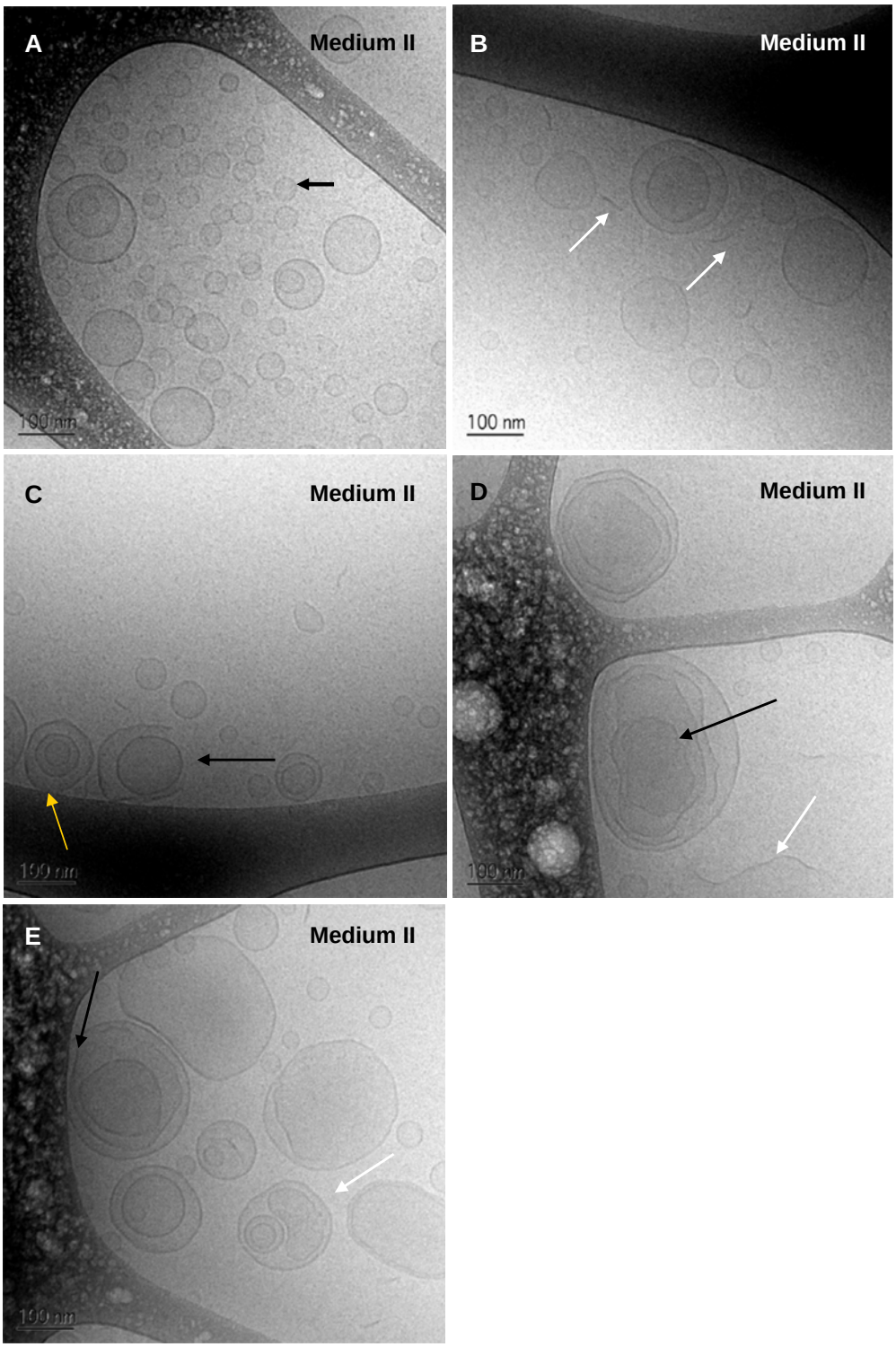

Fig. 3. Cryo-TEM micrographs of biorelevant media. All micrographs are taken from medium II (BS/PL/MG/FA, 15:3.75:7.5:15). Unilamellar (indicated by *black arrow*) and bilamellar or tri-lamellar vesicles are depicted at **a**–**c**. A ruptured bilamellar vesicle is present in **c** (indicated by *black arrow*) close to an open bilamellar vesicle (indicated by *yellow arrow*). Bilayer fragments are occasionally present (**a**–**c**) (indicated by *white arrows*). Vesicles contained internal deformed structures were observed (**d**, **e**) (indicated by *black arrows*). Undulations and ripples are present on the bilayers in the inner part of the vesicles. A multi-compartment vesicle was observed (**e**) (indicated by *white arrow*). The micelles are present as *small dots*. Scale bar represents 100 nm.

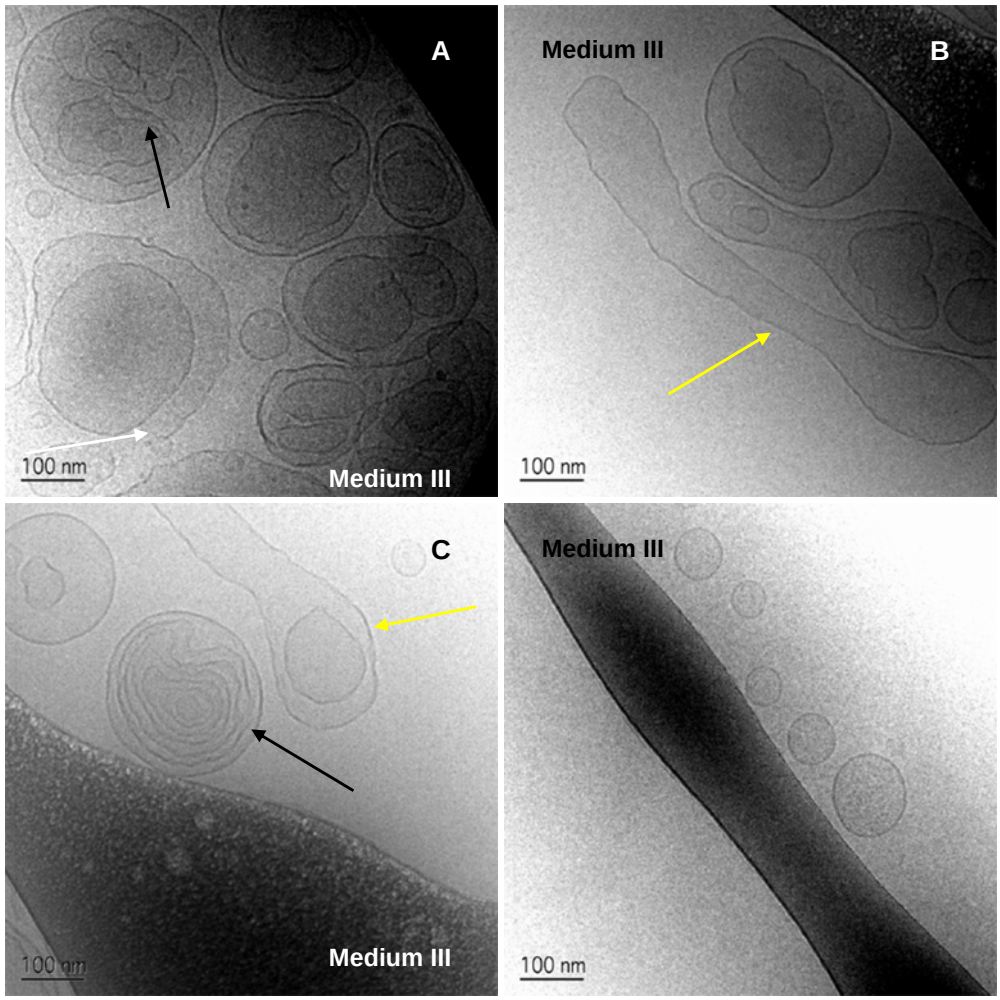

Fig. 4. Cryo-TEM micrographs of biorelevant media. All micrographs are taken from medium III (BS/PL/MG/FA, 15:3.75:10:20). Vesicles containing internal deformed structures with undulations and ripples present on the bilayers in the inner part of the vesicles are depicted (**a**, indicated by *black arrow*). A disrupted vesicle membrane is visible (**a**, indicated by *white arrow*). Elongated or microtubules are depicted as well (**b**, **c**, indicated by *yellow arrows*). A multivesicular structure with rippled bilayers is depicted at **c** (indicated by *black arrow*). Unilamellar vesicles less than 100 nm were present at low numbers (**d**). Scale bar represents 100 nm.

(Fig. 5e, indicated by black arrow) were present. In some cases vesicles are elongated (Fig. 5d). Due to their high absolute ζ-potential values no aggregation was noticed among the vesicles in the same manner as in medium II and III.

The structures observed in the current study are in broad agreement with previous reports where model lipid systems containing monoglycerides, oleic acid and sodium taurodeoxycholic acid were visualized by freeze fracture electron microscopy (17). In samples with high concentrations of lipolytic products, unilamellar and multilamellar vesicles were visualized. Additionally, fatty acids have demonstrated their ability to form unilamellar vesicles upon dispersion in aqueous solutions (47). Consequently, the following question arises: What are the main components in these colloidal phases? It can be assumed that monoglycerides, fatty acids and phosphatidylcholine are present in these structures. These colloidal phases closely resemble phospholipid liposomes in their structure and morphological properties. Furthermore, it should be emphasized that there is the possibility that vesicles exceeding diameters of 1 μm could be formed, but these cannot be visualized due to limitations of the Cryo-TEM method.

Fed State *In Vitro* Lipolysis

Lipolysis Rate of SNEDDS Formulation

The lipolysis rate of the SNEDDS formulation is depicted in Fig. 6. The consumption of NaOH reflects the progress of lipolysis. The values presented have been corrected by subtracting the amount of NaOH consumed when the experiment was carried out without any formulation present. After 30 min almost 42% of the lipid formulation was hydrolyzed.

Zeta Potential During In Vitro Lipolysis

The ζ-potential of the intermediate lipolysis products was studied over time (Fig. 7). Five minutes after initiation of lipolysis, the ζ-potential decreased sharply

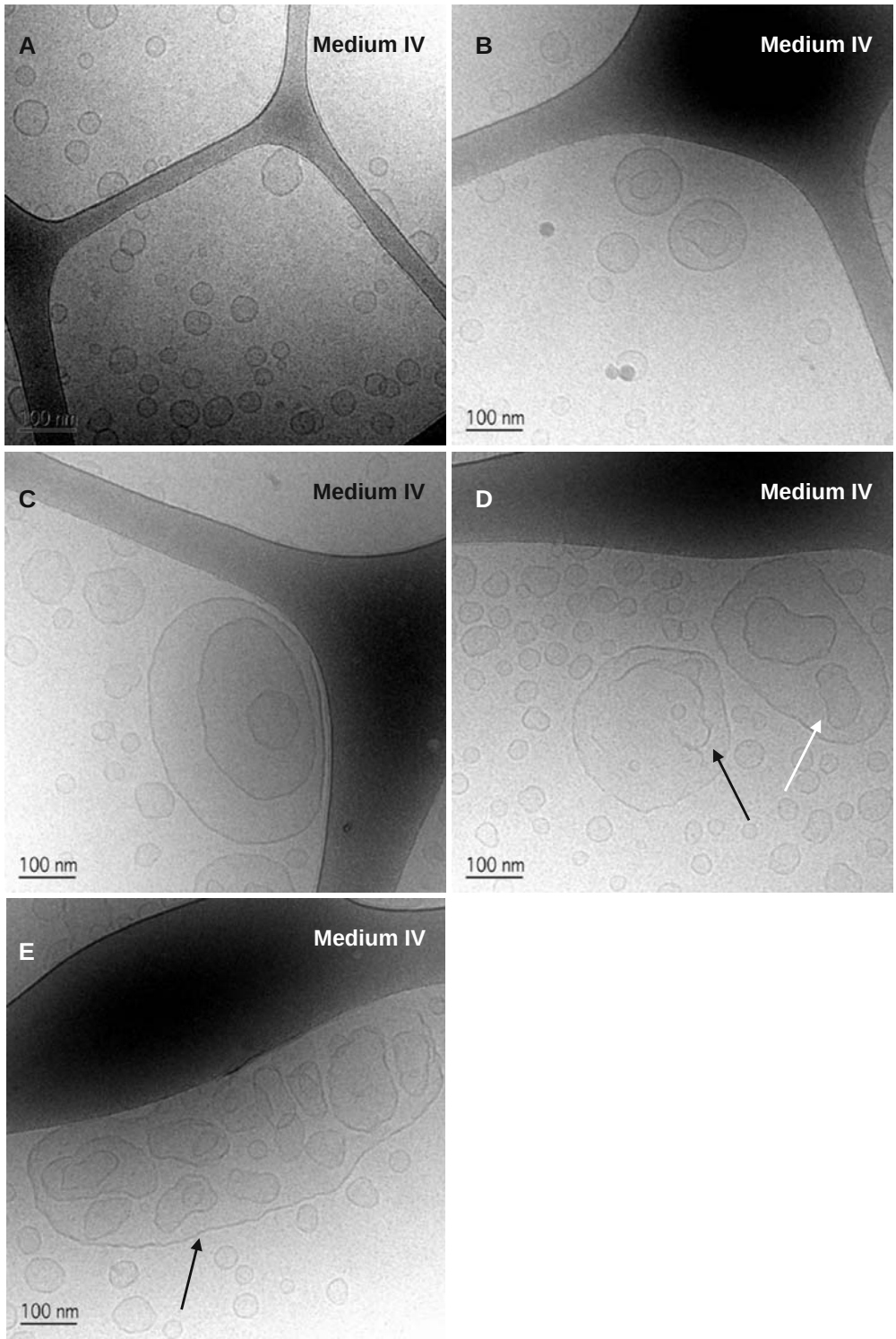

Fig. 5. Cryo-TEM micrographs of biorelevant media. All micrographs are taken from medium IV (BS/PL/MG/FA, 20:5:10:20). Unilamellar, bilamellar or tri-lamellar vesicles are present (**a**–**c**). Big multi-compartment vesicles were present containing large bilayer fragments (**d**, indicated by *black arrow*), vesicles (**d**, indicated by white arrow), or even a cluster of vesicles with undulations and ripples within a large bilayer (**e**, indicated by *black arrow*). Scale bar represents 100 nm.

from−13 to −16 mV. This low level was maintained for the remaining 30 min of lipolysis. These changes advocate interactions between the micelles and the surface of the hydrolyzing SNEDDS droplets (e.g. production of fatty acids).

Furthermore, calcium ions are also expected to shield the surface of the oil droplets with positively charged ions rendering the ζ-potential of the droplets less negative. The ζ-potential values during *in vitro* lipolysis of the SNEDDS

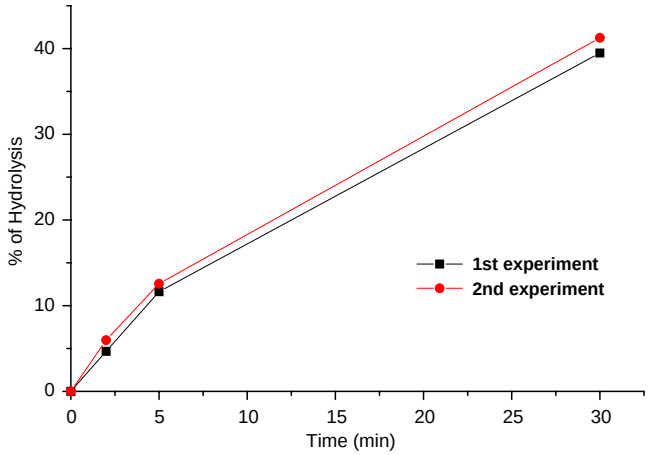

Fig. 6. Percentage of initial triacylglycerol hydrolyzed at different time points as determined from the number of OH^- ions present in the titrant. The values presented in the graph are corrected by subtracting the amount of NaOH consumed when the experiment was carried out only with medium (without formulation) $n=2$.

formulation at high level BS/PL conditions follow the same profile as at low level BS/PL conditions (32) but the measurements in absolute values are higher for the first one.

Moreover, the ζ-potential values of the biorelevant media are significantly higher compared with the values obtained from the lipolysis studies. This is probably due to the addition of calcium ions during lipolysis. Calcium significantly reduces the overall charge of the lipid digestion products.

Cryo-TEM Studies

Visualization of Structures Generated During In Vitro Lipolysis of Snedds at Fed State Conditions

The results presented here are the outcome of two experiments of 70 images in total.

At the beginning of the lipolysis (0 min) spherical emulsion droplets are formed upon dispersion of the SNEDDS precursor in the lipolysis medium (Fig. 8a, indicated by black arrows) exceeding diameters up to 100 nm. Micelles are present as well and can be seen as small dots. After 2 min (or 5% of hydrolysis) multilamellar vesicles (vesicles containing internal deformed structures and oil droplets)were observed (Fig. 8b–d).

Undulations and ripples are present on the bilayers in the inner part of the vesicles in the same manner as observed for the biorelevant media. Previously, similar types of structures have been reported when cubosomes (binary system of monoolein MO-H_2O) were incubated with a microbial lipase (*Thermomyces lanuginose*; 48).

Irregular vesicles with inner structures were formed in the presence of lipase. Moreover, milk lipid membrane vesicles (containing among the other components monoglycerides and fatty acids) show the same morphology as the vesicles visualized in the current study (49). When 15% of the lipid material is hydrolysed (5 min) oil droplets (indicated by black arrow) and lipid bilayer (indicated by white arrow) are visualized (Fig. 8e).

The large multivesicullar structures shown in Fig. 8b,c are replaced by multilamellar vesicles (Fig. 8f), non-organized material, unilamellar vesicles (Fig. 8g) and bending lipid bilayers (Fig. 8h).

Fig. 8. Cryo-TEM micrographs of *in vitro* lipid digestion of SNEDDS formulation at fed state. **a** Cryo-TEM micrographs of oil droplets and micelles at time point 0. Shows oil droplets (OD) of different sizes (*black arrows*) in the lipolysis medium (fed state) containing pancreatic lipase 800 USP together with micelles. Scale bar represents 100 nm. **b–d** Cryo-TEM micrographs of lipolytic products 2 min after the addition of the lipase. **b** Shows multilamellar vesicles. Undulations and ripples are present on the bilayers in the inner part of the vesicles. The inner bilayers appear perforations (indicated by *black arrows*). Open vesicles (indicated by *white arrow*) and lipid monolayers can be observed (indicated by *yellow arrows*). Aggregated material [protein] (*asterisk*) originating from the lipase. **b** Vesicles contained internal deformed structures. **c** Oil droplets (indicated by *black arrow*) and micelles depicted are as black dots are present Scale bar represents 100 nm. **e–i** Cryo-TEM micrographs of lipolytic products 5 min after the addition of the lipase. Oil droplets (indicated by *black arrow*) and lipid bilayer (indicated by *white arrow*) are visualized (**e**). Multilamellar vesicles and lipid monolayers are present (**f**). Bilamellar vesicle close to non-organised lipid material (**g**). Lipid bilayers aligned parallel to each other (**h**). Micelles are present as black dots (indicated by *black arrow*) (**g**). Large bilayer fragment and micelles (**i**). Scale bar represents 100 nm. **j**. Cryo-TEM micrographs of lipolytic products 30 min after the addition of the lipase. Ladder shape structures (indicated by *black arrow*) and aggregated material. These structures were quite long (several μm) and had a width of approximately 100 nm. Scale bar represents 500 nm.

Micelles are present during the whole process. Their morphology has similarities with other micellar systems that have been identified and reported previously (50). As documented earlier (32), after 30 min (40% of hydrolysis) only micelles and material originated from the pancreatic lipase could be detected (Fig. 8j). It should be emphasized that striking changes occur at the beginning of the reaction (up to 5 min). These results are in agreement with our previous study (32) visualizing the same SNEDDS formulation at fasted state BS/PL levels. In that study structural changes were recorded in the same time frame (5 min).

Hydrolysis of phospholipid in vesicles to free fatty acids and lysophospholipids by phospholipase A_2 (PLA_2) was visualized by Cryo-TEM. The study revealed the formation of perforated vesicles. Over time, these perforated vesicles converted into bilayer fragments, micelles and open vesicles in a similar manner as in the present study (51).

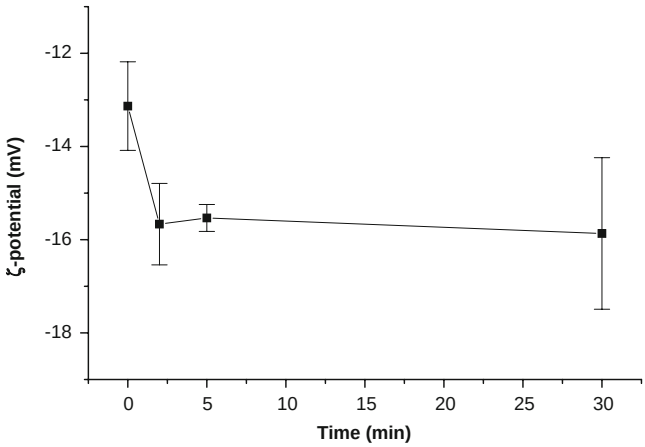

Fig. 7. ζ-potential values as a function of time during lipid digestion for the SNEDDS formulation. All measurements performed at 37°C. These are the mean values±SD of three different experiments.

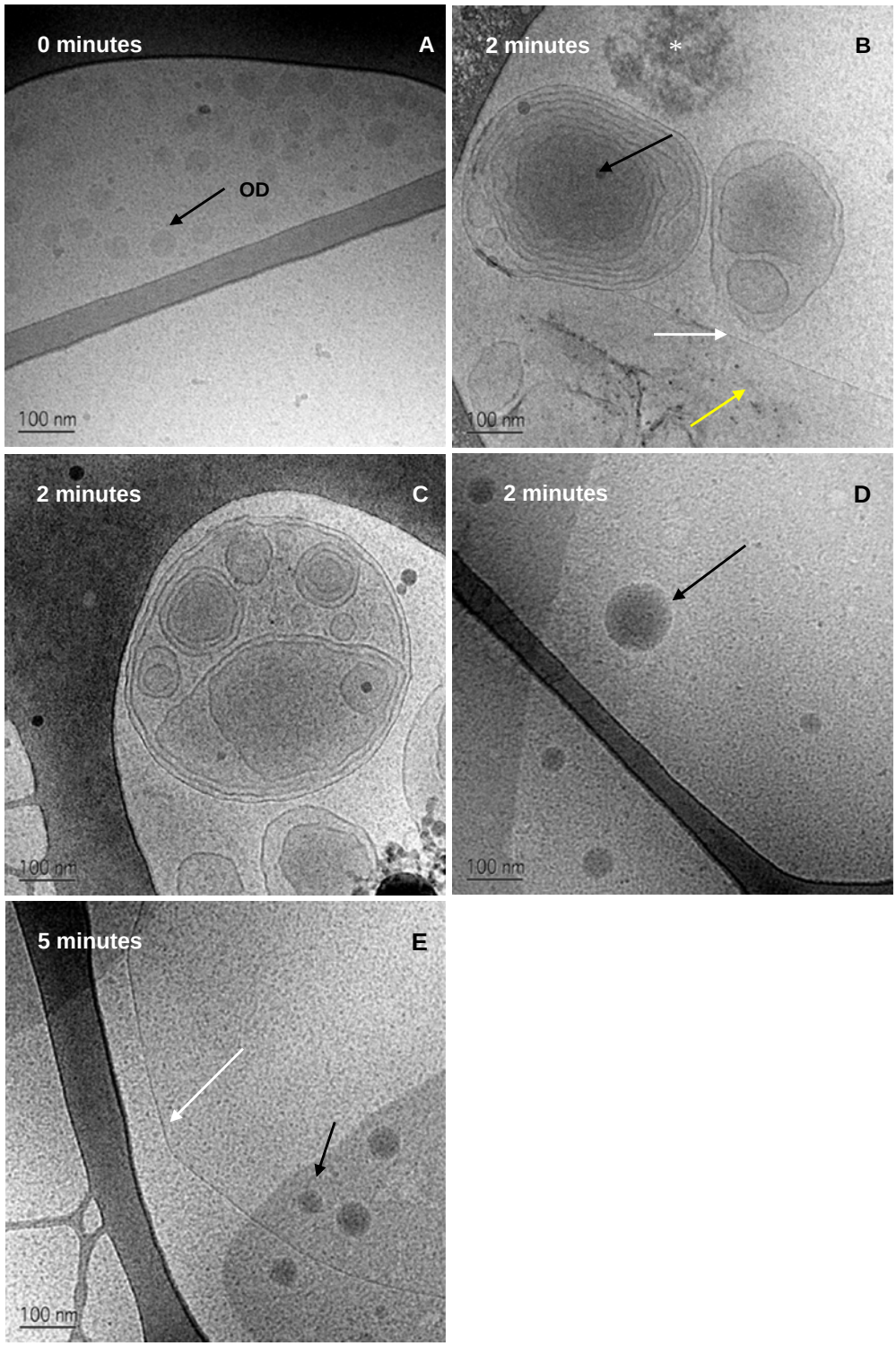

It is believed that the mechanism of lipolysis includes the accumulation of different kinds of polar lipids on the surface of the oil droplet as a result of the hydrolysis by pancreatic lipase (52). This lipid material (mainly monoglycerides and fatty acids) will facilitate the formation of multilamellar liquid crystalline phases on the surface droplet which are gradually "detached" from the surface and produce either multi or unilamellar vesicles and finally upon further interaction with bile salts, to mixed micelles (17,31).

The sequence of events presented in the current study is in line with the previous studies (17,31) and our recent study where a SNEDDS formulation was digested at low levels of PL and BS (32).

Summary of the Cryo-TEM Studies

To summarize, the following observations have been made regarding the colloidal structures of biorelevant media:

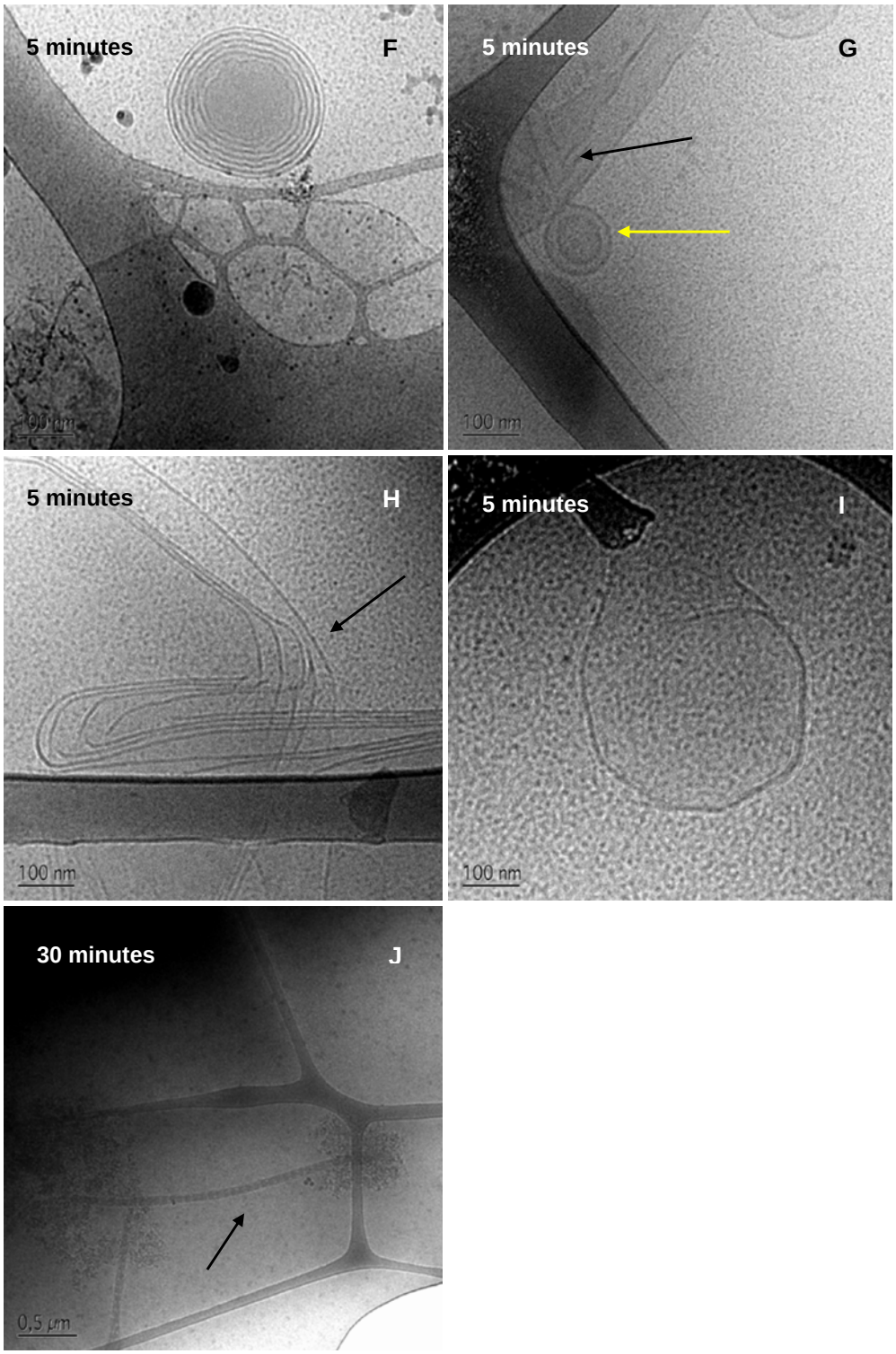

Fig. 8. (continued).

when only BS and PL are present in a ratio of 4:1, only micelles are visualized, even at 15 mM BS. Upon addition of lipolysis products (monoolein and oleic acid) vesicles (either unilamellar or multilamellar), bilayer fragments are formed in addition to the preexisting micelles. Furthermore, in some cases, vesicles with a deformed internal structure are recognized, suggesting surface tension or uneven lateral stress of these particles. Most probably these are intermediate structural features that have not yet reached in equilibrium. This could be partly supported from the fact the smaller colloid structures, up to 100 nm, are mostly well-defined unilamellar and bilamellar vesicles. On the contrary, undulations and rippled bilayers are more common in bigger vesicles or clusters (up to 400 nm in size). These rough and irregular surfaces imply that the vesiculation is a dynamic

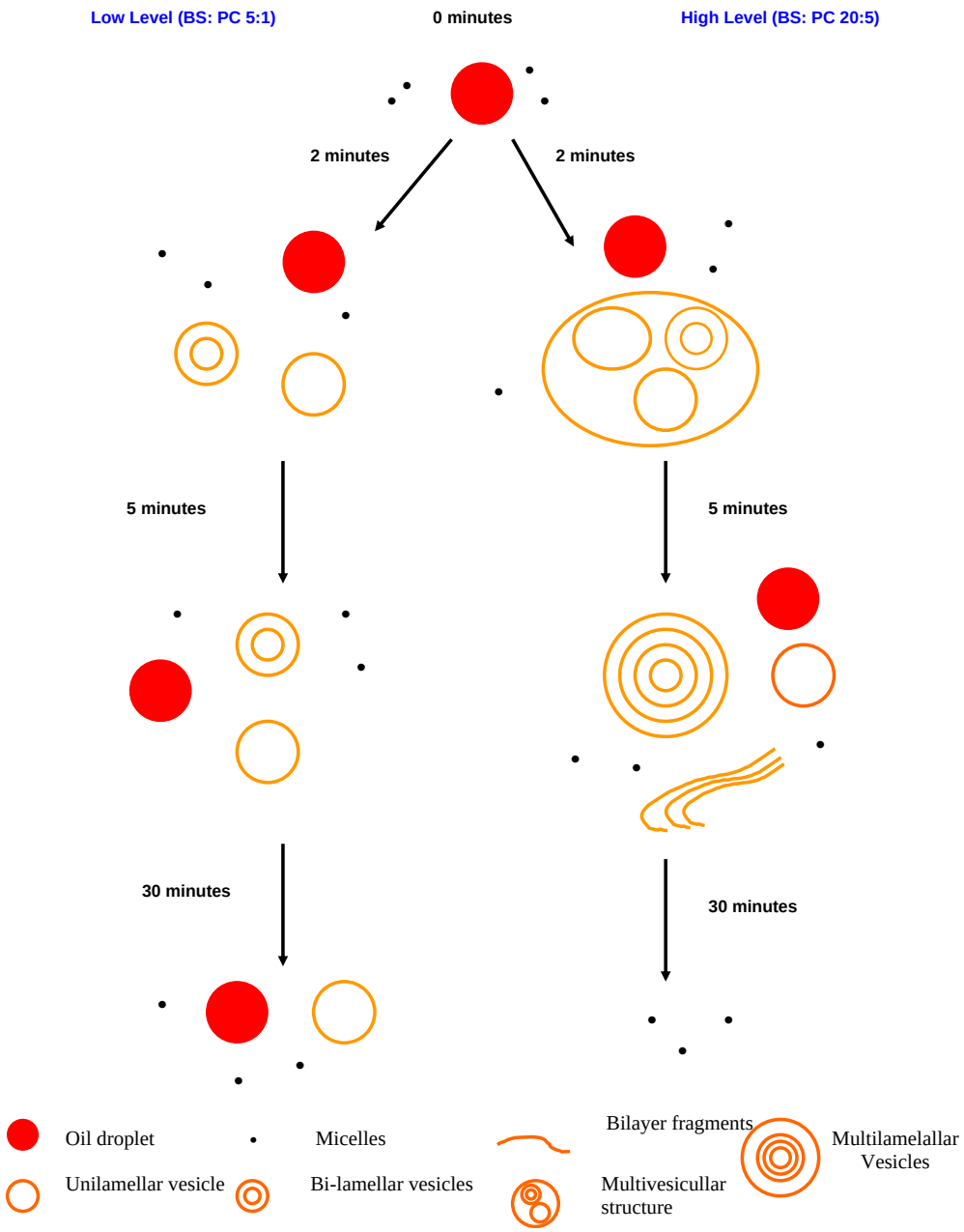

Fig. 9. Morphological evolution of a SNEDDS formulation during lipid digestion in high level and low level of BS/PL ratios. This scheme does not give on the size of the intermediate phases produced during the digestion of the formulation.

process which process is not yet completed. Generally, sharp edges and open vesicles indicate low values of bending elasticity and rather soft bilayers (45).

The impact of vesicles and micelles in colloidal mixtures containing BS, PL and medium and long-chain monoglycerides and fatty acids which represent typical intestinal contents after digestion on the solubilization of poorly soluble drugs has been previously shown (19).

For instance, lipid based formulations that form vesicular structures have increased solubilization capacity for drugs with high LogP values. On the contrary, formulations that lead to the formation of micelles could be advantageous for drugs with low LogP values (19).

The images obtained from *in vitro* digestion of the SNEDDS formulation at fed state are in broad agreement with the vesicular structures visualized from media I, II and III. However, the micelles formed during the *in vitro* lipolysis of the nanoemulsion are very clearly visualized compared with micelles in the biorelevant media that are rather small and less easily recognized. This could also be due to the fact that sodium taurocholate is used for the biorelevant media—while crude bile extract is used for the lipolysis.

The diversity of these vesicles in terms of their size, lamellarity and internal organization could play an important role for solubilization process of poorly soluble drugs (19). Multivesicular structures might have higher loading efficiency

they consist of high numbers of bilayers and lower aqueous volumes.

The impact of vesicle surface charge on drug solubilization is equally important for charge-bearing molecules. The electrical properties of the intermediate colloidal phases can influence their behavior in the biological milieu and their interaction with the gastrointestinal tract. Our data revealed that these intermediate colloidal phases possess a negative surface charge. This might be of importance especially for positively charged drug compounds since the association of the drug and vesicles can be increased due to their electrostatic attractions, eventually leading to higher solubilization capacity. However, it should be emphasized that these values can change during lipid digestion. The presence of calcium shields their surface with positive ions reducing in absolute values the overall ζ-potential, as observed in the case of lipid digestion of a SNEDDS formulation.

In a recent study, we visualized the lipolysis of the same SNEDDS formulation at low level BS/PL concentrations (32). Fig. 9 presents a general scheme of the structures formed during lipid digestion of a SNEDDS formulation during high level (current state) and low level BS/PL ratios (32). Comparing the two studies, the following conclusions can be extracted: (1) multivesicullar structures are dominating structures at high level BS/PL conditions, whereas unilamellar vesicles and bilamellar vesicles are dominating at low level BS/PL conditions (32). This could possibly be explained from the higher amount of PC present at high level BS/PL conditions. This favors the formation of multilamellar structures. (2) In both cases, micelles are present during the entire process. This is despite the difficulty in determining the exact size of these micelles. (3) Higher absolute ζ-potential measurements obtained high level BS/PL conditions. This can be attributed to higher levels of bile salts; since bile salts possess a negative charge in mixtures with PC (38) at pH 6.5. And (4) a lower % of hydrolysis was obtained in high level BS/PL conditions (40%) compared to low level BS/PL conditions (50%).

Previously, it has been shown that the presence of PC in bile salt micelles inhibited the activity of pancreatic lipase by partition of PC molecules between the emulsion interface and the aqueous phase (53). Hence, the higher hydrolysis values at low level BS/PL conditions could be due to smaller amount of PC in the medium (28). The current results are in line with previous studies where high BS/PL (20:5 mM) contained a larger proportion of vesicular structures resulting in higher solubilization capacity for poorly soluble drugs (19).

The fact that the intermediate colloidal phases are negatively charged implies possible interactions with drugs that can be ionized (preferably positively charged).

CONCLUSIONS

Summarizing the findings of the current study we may conclude the following: (1) The biorelevant media form complicated structures comprising vesicles (either unilamellar or multilamellar), bilayer fragments, micelles or even vesicles with an internal deformed structures. (2) The structures visualized during lipid digestion of the nanoemulsion at high level BS/PL conditions are in good agreement with the biorelevant media containing comparable levels of lipid hydrolysis products.

More studies are needed in order to understand the lipolysis of lipid based drug delivery systems and the impact of different excipients. Furthermore, model compounds with different physicochemical properties (e.g. LogD) need to be included in the studies in order to determine the impact of these media to the solubility of drugs in order to fully elucidate the mechanism of action of the biorelevant media and the lipolytic products.

The results obtained from the lipid digestion of the SNEDDS formulation combined with the studies for the biorelevant media suggest that Cryo-TEM studies can offer important information to lipid digestion process of lipid based drug delivery systems. Finally the electrical properties of the lipolytic products combined with the physicochemical properties (e.g. pK_a) of the active compounds loaded to formulation might offer information for possible association of the drugs with these media. The knowledge of composition and characteristics of human intestinal fluids are expanding, therefore there is a precious need for more studies, including physicochemical characterization, of media simulating the human intestinal fluids (54,55). Obviously, a sound knowledge of the mechanism of action of these intermediate colloidal phases is necessary in order to develop and optimize new lipid based drug delivery systems.

ACKNOWLEDGEMENTS

The Cryo-microscopy was performed at the Biomicroscopy unit at the Centre of Chemistry and Chemical Engineering at Lund University. The authors are grateful to Mrs. Gunnel Karlsson for her skilful assistance with the Cryo-TEM instrument. This work was financially supported from Drug Research Academy (DRA), The Danish University of Pharmaceutical Sciences. Mrs IW was an IASTE student at the Danish University of Pharmaceutical Sciences.

REFERENCES

1. T. R. Bates, M. Gibaldi, and J. L. Kanig. Solubilising properties of bile salt solutions. II. Effect of inorganic electrolyte, lipids, and a mixed bile salt system on solubilisation of glutethimide, griseofulvin, and hexestrol. *J. Pharm. Sci.* **55**:901–906 (1966) doi:10.1002/jps.2600550906.
2. T. R. Bates, S. L. Lin, and M. Gibaldi. Solubilisation and rate of dissolution of drugs in the presence of physiologic concentrations of lysolecithin. *J. Pharm. Sci.* **56**:1492–1495 (1967) doi:10.1002/jps.2600561123.
3. L. Martis, N. A. Hall, and A. L. Thakkar. Micelle formation and testosterone solubilisation by sodium glycocholate. *J. Pharm. Sci.* **61**:1757–1761 (1972) doi:10.1002/jps.2600611113.
4. M. Rosoff, and A. T. M. Serajuddin. Solubilisation of diazepam in bile-salts and in sodium cholate–lecithin–water phases. *Int. J. Pharm.* **6**:137–146 (1980) doi:10.1016/0378-5173(80)90086-1.
5. M. A. Kassem, A. G. Mattha, A. E. M. Elnimr, and S. M. Omar. Study of the influence of sodium taurocholate (stc) and sodium glycocholate (sgc) on the mass-transfer of certain drugs—digoxin. *Int. J. Pharm.* **12**:1–9 (1982) doi:10.1016/0378-5173(82)90128-4.
6. A. T. Serajuddin, P. C. Sheen, D. Mufson, D. F. Bernstein, and M. A. Augustine. Physicochemical basis of increased bioavailability of a poorly water-soluble drug following oral administration as organic solutions. *J. Pharm. Sci.* **77**:325–329 (1988) doi:10.1002/jps.2600770409.
7. M. Armand, P. Borel, B. Pasquier, C. Dubois, M. Senft, M. Andre, J. Peyrot, J. Salducci, and D. Lairon. Physicochemical

characteristics of emulsions during fat digestion in human stomach and duodenum. *Am. J. Physiol.* **271**:G172–G183 (1996).
8. A. Tangerman, A. van Schaik, and E. W. van der Hoek. Analysis of conjugated and unconjugated bile acids in serum and jejunal fluid of normal subjects. *Clin. Chim. Acta*. **159**:123–132 (1986) doi:10.1016/0009-8981(86)90044-6.
9. E. Galia, E. Nicolaides, D. Hörter, R. Löbenberg, C. Reppas, and J. B. Dressman. Evaluation of various dissolution media for predicting *in vivo* performance of class I and II drugs. *Pharm. Res*. **15**:698–705 (1998) doi:10.1023/A:1011910801212.
10. B. L. Pedersen, A. Mullertz, H. Brondsted, and H. G. Christensen. A comparison of the solubility of danazol in human and simulated gastrointestinal fluids. *Pharm. Res*. **7**:891–894 (2000) doi:10.1023/A:1007576713216.
11. S. D. Ladas, P. E. Isaacs, G. M. Murphy, and G. E. Sladen. Comparison of the effects of medium and long chain triglyceride containing liquid meals on gall bladder and small intestinal function in normal man. *Gut*. **25**:405–411 (1984) doi:10.1136/gut.25.4.405.
12. E. M. Persson, A. S. Gustafsson, A. S. Carlsson, R. G. Nilsson, L. Knutson, P. Forsell, G. Hanisch, H. Lennernas, and B. Abrahamsson. The effects of food on the dissolution of poorly soluble drugs in human and in model small intestinal fluids. *Pharm. Res*. **12**:2141–2151 (2005) doi:10.1007/s11095-005-8192-x.
13. J. E. Staggers, O. Hernell, R. J. Stafford, and M. C. Carey. Physical–chemical behaviour of dietary and biliary lipids during intestinal digestion and absorption. 1. Phase behaviour and aggregation states of model lipids systems patterned after aqueous duodenal contents of healthy adult human beings. *Biochemistry*. **29**:2028–2040 (1990) doi:10.1021/bi00460a011.
14. O. Hernell, J. E. Staggers, and M. C. Carey. Physicochemical behaviour of dietary and biliary lipids during intestinal digestion and absorption. 2. Phase behaviour and aggregation states of luminal lipids during duodenal fat digestion in health adult human beings. *Biochemistry*. **29**:2041–2056 (1990) doi:10.1021/bi00460a012.
15. S. D. Mithani, V. Bakatselou, C. N. TenHoor, and J. B. Dressman. Estimation of the increase in solubility of drugs as a function of bile salt concentration. *Pharm. Res*. **13**:163–167 (1996) doi:10.1023/A:1016062224568.
16. T. S. Wiedmann, W. Liang, and L. Kamel. Solubilisation of drugs by physiological mixtures of bile salts. *Pharm. Res*. **19**:1203–1208 (2002) doi:10.1023/A:1019858428449.
17. T. S. Wiedmann, and L. Kamel. Examination of the solubilisation of drugs by bile salt micelles. *J. Pharm. Sci*. **91**:1743–1764 (2002) doi:10.1002/jps.10158.
18. D. Ilardia-Arana, H. G. Kristensen, and A. Mullertz. Biorelevant dissolution media: aggregation of amphiphiles and solubility of estradiol. *J. Pharm. Sci*. **95**:248–255 (2006) doi:10.1002/jps.20494.
19. G. A. Kossena, B. J. Boyd, C. J. H. Porter, and W. N. Charman. Separation and characterization of the colloidal phases produced on digestion of common formulation lipids and assessment of their impact on the apparent solubility of selected poorly water-soluble drugs. *J. Pharm. Sci*. **92**:634–648 (2003) doi:10.1002/jps.10329.
20. G. A. Kossena, W. N. Charman, B. J. Boyd, and C. J. H. Porter. Influence of the intermediate digestion phases of common formulation lipids on the absorption of a poorly water-soluble drug. *J. Pharm. Sci*. **94**:481–492 (2005) doi:10.1002/jps.20260.
21. K. J. MacGregor, J. K. Embleton, J. E. Lacy, A. E. Perry, L. J. Solomon, H. Seager, and C. W. Pouton. Influence of lipolysis on drug absorption from the gastro-intestinal tract. *Adv. Drug Deliv. Rev*. **25**:33–46 (1997) doi:10.1016/S0169-409X(96)00489-9.
22. P. Vinson, Y. Talmon, and A. Walter. Vesicle-micelle transition of phosphatidylcholine and octyl glucoside elucidated by cryo-transmission electron microscopy. *Biophys. J*. **56**:669–681 (1989).
23. A. Walter, P. K. Vinson, A. Kaplun, and Y. Talmon. Intermediate structures in the cholate-phosphatidylcholine vesicle–micelle transition. *Biophys. J*. **60**:1315–1325 (1991).
24. J. R. Bellare, H. T. Davis, L. E. Scriven, and Y. Talmon. Controlled environment vitrification system. An improved sample preparation technique. *J. Electron Microsc. Tech*. **10**:87–111 (1988) doi:10.1002/jemt.1060100111.
25. J. Dubochet, M. Adrian, J. Chang, J. C. Homo, J. Lepault, A. W. McDowell, and P. Schultz. Cryo-electron microscopy of vitrified specimens. *Q. Rev. Biophys*. **21**:129–228 (1988).
26. N. H. Zangenberg, A. Müllertz, H. G. Kristensen, and L. Hovgaard. A dynamic *in vitro* lipolysis model. I. Controlling the rate of lipolysis by continuous addition of calcium. *Eur. J. Pharm. Sci*. **14**:115–122 (2001) doi:10.1016/S0928-0987(01)00169-5.
27. N. H. Zangenberg, A. Müllertz, H. G. Kristensen, and L. Hovgaard. A dynamic *in vitro* lipolysis model. II. Evaluation of the model. *Eur. J. Pharm. Sci*. **14**:237–244 (2001) doi:10.1016/S0928-0987(01)00182-8.
28. J. S. Patton, and M. C. Carey. Watching fat digestion. *Science*. **204**:145–148 (1979) doi:10.1126/science.432636.
29. J. S. Patton, R. D. Vetter, M. Hamosh, B. Borgstrom, M. Lindstrom, and M. C. Carey. The light microscopy of triglyceride digestion. *Food Microstruct*. **4**:29–41 (1985).
30. M. W. Rigler, and J. S. Patton. The production of liquid crystalline product by pancreatic lipase in the absence of bile salts. *Biochim. Biophys. Acta*. **751**:444–454 (1983).
31. M. W. Rigler, R. E. Honkanen, and J. S. Patton. Visualization by freeze fracture, *in vitro* and *in vivo*, of the products of fat digestion. *J. Lipid Res*. **8**:836–857 (1986).
32. D. G. Fatouros, B. Bergenstahl, and A. Mullertz. Morphological observations on a lipid based drug delivery system during *in vitro* digestion. *Eur. J. Pharm. Sci*. **31**:85–94 (2007) doi:10.1016/j.ejps.2007.02.009.
33. F. S. Nielsen, E. Gibault, H. Ljusberg-Wahren, L. Arleth, J. S. Pedersen, and A. Müllertz. Characterization of prototype self-nanoemulsifying formulations of lipophilic compounds. *J. Pharm. Sci*. **96**:876–892 (2007) doi:10.1002/jps.20673.
34. Y. Gargouri, H. Moreau, and R. Verger. Gastric lipases: Biochemical and physiological studies. *Biochim. Biophys. Acta*. **1006**:255–271 (1989).
35. J. B. Dressman, R. R. Berardi, L. C. Dermentzoglou, T. L. Russell, S. P. Schmaltz, J. L. Barnett, and K. M. Jarvenpaa. Upper gastrointestinal (GI) pH in young, healthy men and women. *Pharm. Res*. **7**:756–761 (1990) doi:10.1023/A:1015827908309.
36. F. Carriere, J. A. Barrowman, R. Verger, and R. Laugier. Secretion and contribution to lipolysis of gastric and pancreatic lipases during a test meal in humans. *Gastroenterology*. **105**:876–888 (1993).
37. USP 26, The United States Pharmacopoeia/The National Formulary, (USP 26/NF 21). United States Pharmacopoeia Convection, Inc., Rockville (2003).
38. M. Wickham, M. Garrood, J. Leney, P. D. G. Wilson, and A. Fillery-Travis. Modification of phospholipids by bile salt: Effect on pancreatic lipase activity. *J. Lipid Res*. **39**:623–632 (1998).
39. D. Paolino, C. A. Ventura, S. Nistico, G. Puglisi, and M. Fresta. Lecithin microemulsions for the topical administration of ketoprofen: Percutaneous adsorption through human skin and *in vivo* human skin tolerability. *Int. J. Pharm*. **244**:21–31 (2002) doi:10.1016/S0378-5173(02)00295-8.
40. M. N. Jones. he surface properties of phospholipid liposome systems and their characterization. *Adv. Colloid Interface Sci*. **54**:93–128 (1995) doi:10.1016/0001-8686(94)00223-Y.
41. S. McLaughlin, N. Mulrine, T. Gresalfi, G. Vaio, and A. McLaughlin. Adsorption of divalent cations to bilayer membranes containing phosphatidylserine. *J. Gen. Physiol*. **77**:445–473 (1981) doi:10.1085/jgp.77.4.445.
42. R. Schubert, and K. H. Schmidt. Structural changes in vesicle membranes and mixed micelles of various lipid compositions after binding of different bile salts. *Biochemistry*. **27**:8787–8794 (1988) doi:10.1021/bi00424a015.
43. M. T. Paternostre, M. Roux, and J. L. Rigaud. Mechanisms of membrane protein insertion into liposomes during reconstitution procedures involving the use of detergents. 1. Solubilisation of large unilamellar liposomes (prepared by reverse-phase evaporation) by triton X-100, octyl glucoside, and sodium cholate. *Biochemistry*. **27**:2668–2677 (1988) doi:10.1021/bi00408a006.
44. M. Kokkona, P. Kallinteri, D. Fatouros, and S. G. Antimisiaris. Stability of SUV liposomes in the presence of cholate salts and pancreatic lipases: effect of lipid composition. *Eur. J. Pharm. Sci*. **9**:245–252 (2000) doi:10.1016/S0928-0987(99)00064-0.

45. D. D. Lasic, R. Joannic, B. C. Keller, P. M. Frederik, and L. Auvrey. Spontaneous vesiculation. *Adv. Colloid Interface Sci*. **89–90**:337–349 (2001) doi:10.1016/S0001-8686(00)00067-1.
46. R. Waninge, T. Nylander, M. Paulsson, and B. Bergenstahl. Milk membrane lipid vesicle structures studied with Cryo-TEM. *Colloids Surf. B Biointerf*. **31**:257–264 (2003) doi:10.1016/S0927-7765(03)00145-0.
47. W. R. Hargreaves, and D. W. Deamer. Liposomes from ionic, single-chain amphiphiles. *Biochemistry*. **17**:3759–3768 (1978) doi:10.1021/bi00611a014.
48. J. Borne, T. Nylander, and A. Khan. Effect of lipase on monoolein-based cubic phase dispersion (cubosomes) and vesicles. *J. Phys. Chem. B*. **106**:10492–10500 (2002) doi:10.1021/jp021023y.
49. R. Waninge, E. Kalda, M. Paulsson, T. Nylander, and B. Bergenstahl. Cryo-TEM of isolated milk fat globule membrane structures in cream. *Phys. Chem. Chem. Phys*. **6**:1518–1523 (2004) doi:10.1039/b314613h.
50. J. Gustafsson, T. Nylander, M. Almgren, and H. Ljusberg-Wahren. Phase behaviour and aggregate structure in aqueous mixtures of sodium cholate and glycerol monooleate. *J. Coll. Inter. Sci*. **211**:326–335 (1999) doi:10.1006/jcis.1998.5996.
51. T. H. Calissen, and Y. Talmon. Direct imaging by cryo-TEM shows membrane break-up by phospholipase A2 enzymatic activity. *Biochemistry*. **37**:10987–10993 (1998) doi:10.1021/bi980255d.
52. K. J. MacGregor, J. K. Embleton, J. E. Lacy, E. A. Perry, L. J. Solomon, H. Seager, and C. W. Pouton. Influence of lipolysis on drug absorption from the gastro-intestinal tract. *Adv. Drug Deliv. Rev*. **1**:33–46 (1997) doi:10.1016/S0169-409X(96)00489-9.
53. J. S. Patton, and M. C. Carey. Inhibition of human pancreatic lipase-colipase activity by mixed bile salt-phospholipid micelles. *Am. J. Physiol*. **241**:G328–G336 (1981).
54. J. Jantratid, N. Janssen, C. Reppas, and J. B. Dresmman. Dissolution media simulating conditions in the proximal human gastrointestinal tract: An update. *Pharm. Res*. **25**:1663–1676 (2008) doi:10.1007/s11095-008-9569-4.
55. S. Clarysse, J. Tack, F. Lammert, G. Duchateau, C. Reppas, and P. Augustijns. Postprandial evolution in composition and characteristics of human duodenal fluids in different nutritional states. *J. Pharm. Sci*. (2008) doi:10.1002/jps.21502.